Report

Cell Reports

# Carnitine Palmitoyltransferase 1A Has a Lysine Succinyltransferase Activity

## Graphical Abstract

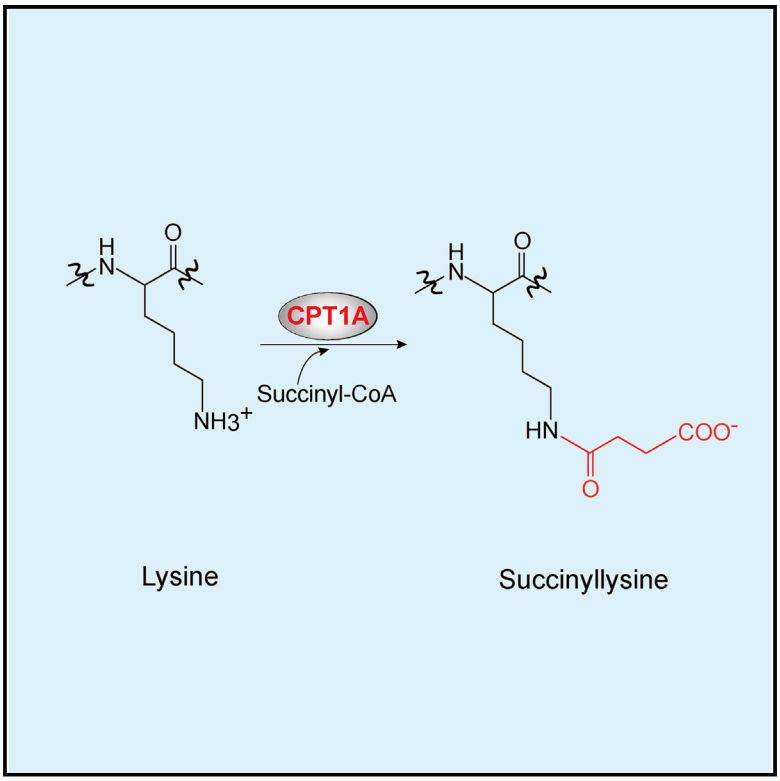


## Authors

Kiran Kurmi, Sadae Hitosugi, Elizabeth K. Wiese, ..., Larry M. Karnitz, Matthew P. Goetz, Taro Hitosugi

## Correspondence

hitosugi.taro@mayo.edu

## In Brief

Kurmi et al. find that carnitine palmitoyltransferase (CPT) 1A has lysine succinyltransferase (LSTase) activity *in vivo* and *in vitro*. Mutation of CPT1A Gly710 (G710E) selectively inactivates canonical carnitine palmitoyltransferase (CPTase) activity but not LSTase activity.

## Highlights

- CPT1A succinylates proteins *in vitro* using succinyl-CoA as a substrate
- CPT1A increases lysine succinylation in cells without altering succinyl-CoA levels
- CPT1A inhibits enolase 1 by lysine succinylation *in vivo* and *in vitro*
- About 100 CPT1A-dependent succinylated proteins were identified

Kurmi et al., 2018, Cell Reports *22*, 1365–1373
February 6, 2018 
https://doi.org/10.1016/j.celrep.2018.01.030

CellPress

Cell Reports
Report



# Carnitine Palmitoyltransferase 1A Has a Lysine Succinyltransferase Activity

Kiran Kurmi,[1,2] Sadae Hitosugi,[3] Elizabeth K. Wiese,[1,2] Felix Boakye-Agyeman,[3,6] Wilson I. Gonsalves,[4] Zhenkun Lou,[1,3] Larry M. Karnitz,[1,3] Matthew P. Goetz,[1,5] and Taro Hitosugi[1,3,7,*]
[1]Department of Molecular Pharmacology and Experimental Therapeutics, Mayo Clinic, Rochester, MN 55905, USA
[2]Mayo Clinic Graduate School of Biomedical Sciences, Mayo Clinic, Rochester, MN 55905, USA
[3]Division of Oncology Research, Mayo Clinic, Rochester, MN 55905, USA
[4]Department of Hematology, Mayo Clinic, Rochester, MN 55905, USA
[5]Division of Medical Oncology, Mayo Clinic, Rochester, MN 55905, USA
[6]Present address: Duke Clinical Research Institute, Durham, NC 27705, USA
[7]Lead Contact
*Correspondence: hitosugi.taro@mayo.edu
https://doi.org/10.1016/j.celrep.2018.01.030

## SUMMARY

**Lysine succinylation was recently identified as a post-translational modification in cells. However, the molecular mechanism underlying lysine succinylation remains unclear. Here, we show that carnitine palmitoyltransferase 1A (CPT1A) has lysine succinyltransferase (LSTase) activity *in vivo* and *in vitro*. Using a stable isotope labeling by amino acid in cell culture (SILAC)-based proteomics approach, we found that 101 proteins were more succinylated in cells expressing wild-type (WT) CPT1A compared with vector control cells. One of the most heavily succinylated proteins in this analysis was enolase 1. We found that CPT1A WT succinylated enolase 1 and reduced enolase enzymatic activity in cells and *in vitro*. Importantly, mutation of CPT1A Gly710 (G710E) selectively inactivated carnitine palmitoyltransferase (CPTase) activity but not the LSTase activity that decreased enolase activity in cells and promoted cell proliferation under glutamine depletion. These findings suggest that CPT1A acts as an LSTase that can regulate enzymatic activity of a substrate protein and metabolism independent of its classical CPTase activity.**

## INTRODUCTION

Multiple post-translational modifications on the epsilon-amino group of lysine regulate protein functions. Recent studies have added lysine succinylation, which has been observed in many species (Colak et al., 2013; Park et al., 2013; Rardin et al., 2013; Weinert et al., 2013; Zhang et al., 2011), as an additional lysine modification. Sirtuin (SIRT) 5 can remove succinyl modifications from lysine (Du et al., 2011). Indeed, recent studies showed that increased accumulation of succinyl-coenzyme A (CoA) caused increased lysine succinylation, likely because of non-enzymatic lysine succinylation (Li et al., 2015; Wagner and Payne, 2013; Weinert et al., 2013). However, given that (1) lysine acetylation is catalyzed by acetyltransferases even though acetyl-CoA can non-enzymatically acetylate lysines (Choudhary et al., 2014) and (2) regulatory post-translational modifications are typically catalyzed by enzymes, it is likely that there is a lysine succinyltransferase (LSTase) that catalyzes the forward reaction of lysine succinylation using succinyl-CoA as a substrate.

Therefore, succinyl-CoA is considered to be a putative substrate for an LSTase. It was also shown, more than 30 years ago, that short-chain dicarboxylic-acyl-CoAs, including succinyl-CoA, bind to carnitine palmitoyltransferase 1A (CPT1A) and inhibit its carnitine palmitoyltransferase (CPTase) activity (McGarry et al., 1977; Mills et al., 1983). CPT1A catalyzes the formation of long-chain acylcarnitines from long-chain acyl-CoAs and carnitine, the rate-limiting step of mitochondrial fatty acid oxidation (FAO) that metabolizes fatty acids into acetyl-CoA to produce ATP in mitochondria. Although the inhibitory effect of succinyl-CoA on CPTase activity is well accepted in the field, how succinyl-CoA binds to CPT1A remains unclear because of the lack of the crystal structure of the CPT1A protein. In this study, we show that CPT1A is able to use succinyl-CoA as a substrate to function as an LSTase *in vitro* and *in vivo*. Our SILAC-based quantitative succinylation proteomics analysis identified 171 lysine sites on 101 proteins (out of 550 lysine sites on 247 proteins total) that were succinylated in a CPT1A expression-dependent manner in cells. Importantly, the CPTase activity and the LSTase activity of CPT1A can be separated by mutation of CPT1A Gly710 (G710E). Using this CPT1A G710E mutant, we show that the LSTase activity of CPT1A inhibited enolase 1 enzymatic activity and promoted cell proliferation under glutamine depletion. Thus, we propose that CPT1A regulates cellular metabolism by succinylating substrate proteins independent of its canonical CPTase activity.

## RESULTS AND DISCUSSION

### Identification of CPT1A as a Potential LSTase

Because succinyl-CoA is a short-chain acyl-CoA, we hypothesized that acyltransferases with CoA binding domains may have LSTase activity. To identify potential candidates, we first searched the Swiss-Prot database using "acyltransferase" and "CoA binding" as keywords and obtained 33 candidate proteins (Figure S1A). We next excluded acyltransferases expressed in

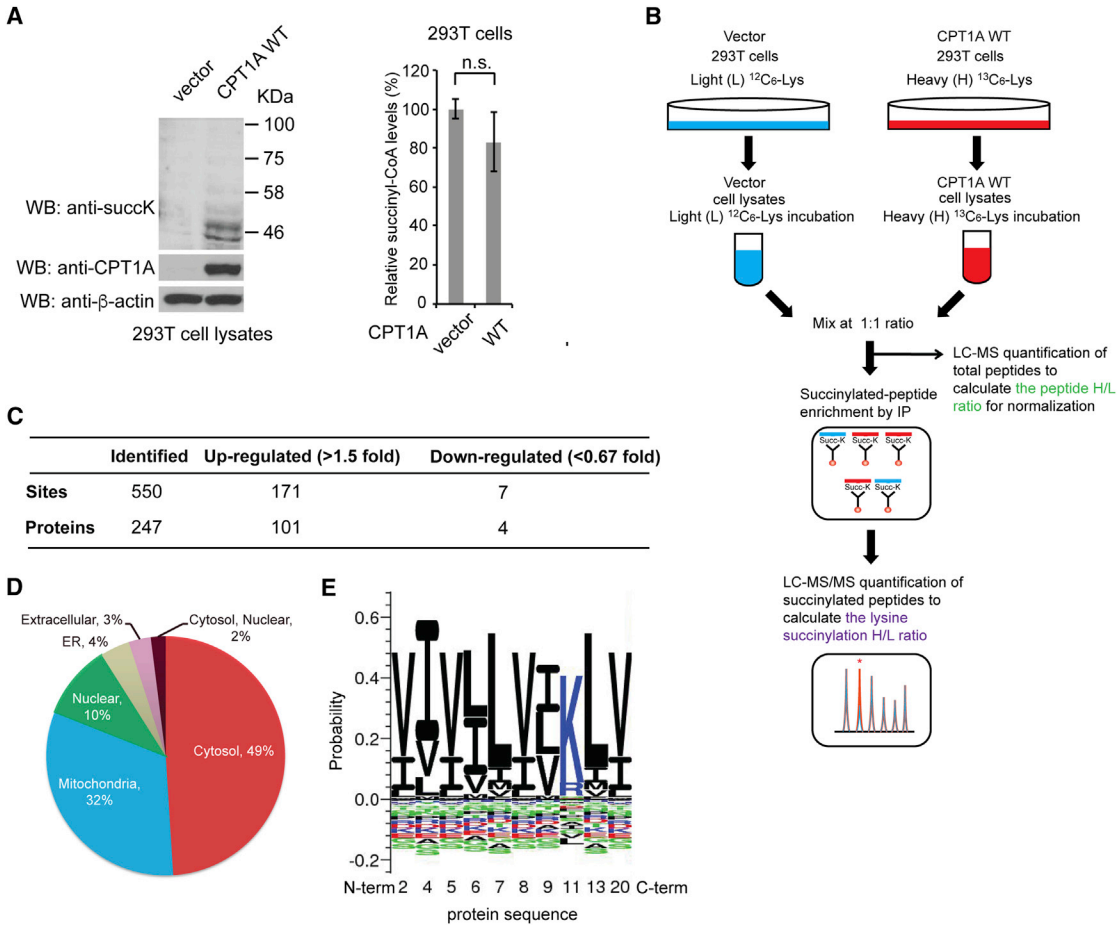


**Figure 1. Identification of CPT1A-Dependent Lysine-Succinylated Proteins Using a SILAC-Based Quantitative Proteomics Approach**

(A) Left: WB of lysates from 293T cells stably expressing vector control and CPT1A WT with anti-pan-succinylated lysine, anti-CPT1A, and anti-β-actin antibodies. Right: GC-MS analysis of succinyl-CoA extracted from 293T cells expressing vector control and CPT1A WT. Error bars, ±SD of three independent measurements. P values were determined using a two-tailed Student's t test. n.s., not significant.

(B) Schematic diagram of the SILAC-based quantitative proteomics approach for the identification of CPT1A-dependent lysine succinylation.

(C) Summary of the quantified lysine-succinylated sites and proteins.

(D) Subcellular distribution of CPT1A-dependent lysine-succinylated proteins.

(E) Consensus sequence motif logo for the amino acid sequences surrounding the 171 CPT1A-dependent succinylated lysine sites (>1.5-fold).

See also Figure S1 and Tables S1 and S2.

yeast, because yeasts do not express desuccinylases (e.g., SIRT5) that would be expected to reverse succinylation catalyzed by an LSTase. After these screening steps, we obtained nine candidates, including all CPT family members (Figure S1A). Among the CPT family members, CPT1A is the most expressed isoform in the liver, where lysine succinylation occurs at highest levels compared with other tissues (Park et al., 2013; Rardin et al., 2013). Interestingly, short-chain dicarboxylic-acyl-CoAs, including succinyl-CoA, are known to inhibit the CPTase activity (McGarry et al., 1977; Mills et al., 1983). A structural modeling study of CPT1A proposed two potential CoA binding pockets within the active site (López-Viñas et al., 2007). Also, lysine succinylation and carnitine acylation are quite different in terms of chemical reactivity and steric occlusion because lysine succinylation is linked to the epsilon-amino group of lysine, whereas carnitine acylation occurs on a secondary hydroxyl group. Thus, we hypothesize that succinyl-CoA may bind to a locus different from the palmitoyl-CoA-binding locus within the CPT1A active site, which triggers CPT1A to have an additional enzymatic activity: the ability to succinylate lysine residues. To examine this hypothesis, we generated human 293T cell lines stably expressing wild-type (WT) human CPT1A and vector control and measured the total lysine succinylation levels in lysates by western blotting (WB) with a pan anti-succinylated lysine antibody. Expression of CPT1A WT increased the total lysine succinylation levels in 293T cell lysates compared with expression of vector control (Figure 1A, left). We next measured intracellular succinyl-CoA levels in 293T cell lines expressing CPT1A WT and vector control by an isotope-ratio-based approach with gas chromatography (GC)/mass spectrometry (MS) as we have performed previously (Hitosugi et al., 2012). The detailed calculations of intracellular succinyl-CoA levels in the cells are

described in Figure S1B. Using this isotope-ratio based approach, we found no significant increase in succinyl-CoA levels by expression of CPT1A WT compared with expression of vector control in 293T cells, indicating that the increase in lysine succinylation by CPT1A WT is not due to higher intracellular succinyl-CoA levels (Figure 1A, right). We also measured $NAD^+$ concentration in vector and CPT1A WT-expressed 293T cells and found no significant change in $NAD^+$ concentration by CPT1A expression (Figure S1C). These results suggest that CPT1A may function as an LSTase in cells. In addition, we sought to investigate whether CPT1A is the specific enzyme that has the observed LSTase activity. We examined lysine succinylation levels in cells expressing another isoform of CPT1 family member CPT1C, which was identified as a potential LSTase from Swiss-Prot search in addition to CPT1A (Figure S1A). We ectopically expressed CPT1C in 293T cells and measured the total lysine succinylation levels in lysates by WB with a pan anti-succinylated lysine antibody. Expression of CPT1C WT did not increase the total lysine succinylation levels in 293T cell lysates compared with expression of vector control (Figure S1D).

## Identification of CPT1A-Dependent Lysine-Succinylated Proteins Using a SILAC-Based Quantitative Proteomics Approach

To identify CPT1A-dependent lysine-succinylated proteins and the sites of succinylation, we next performed quantitative succinylation analysis using stable isotope labeling by amino acid in cell culture (SILAC). 293T cells stably transfected with vector control (vector control cells) were incubated with light (L) [U-12C6]-lysine, while 293T CPT1A WT cells were incubated with heavy (H) [U-13C6]-lysine. Lysates from these two cell lines were mixed in a 1:1 ratio. One half of the mixed lysates was used for quantitative liquid chromatography (LC)-MS analysis for the total peptide normalization, and the other half was used for affinity enrichment by immunoprecipitation with pan anti-succinylated lysine antibody-conjugated beads followed by LC-MS/MS (Figure 1B). We found that succinylation levels of 171 unique lysine sites on 101 proteins (31% of the total 550 detected unique lysine sites on 247 proteins) were increased by more than 1.5-fold in CPT1A WT cells compared with vector control cells (Figure 1C; Tables S1 and S2). These results suggest that CPT1A regulates lysine succinylation in cells. We also investigated the possibility that the increased succinylation bands could be degradation products of expressed CPT1A (Figure 1A). We found no lysine-succinylated CPT1A peptide in our SILAC proteomics data from the CPT1A-expressed 293T cell lysates (Table S1), indicating that the increased succinylation bands by CPT1A expression would appear to be the lysine-succinylated downstream substrate proteins.

Using the SILAC proteomics data, we next examined the subcellular distribution of the CPT1A-dependent lysine-succinylated proteins and assessed whether there is a consensus sequence motif for CPT1A-dependent lysine succinylation. We found that almost 50% of the proteins with greater than a 1.5-fold increase in succinylation were cytosolic proteins (Figure 1D; Table S2). Analysis of the amino acids flanking the 171 succinylated lysines revealed that they were enriched in nonpolar hydrophobic amino acids such as leucine, valine, and isoleucine (Figure 1E; Table S2). These results are in contrast to recent studies on SIRT5 showing that most of the SIRT5-dependent lysine-succinylated proteins were mitochondrial proteins and that succinylated lysine sites targeted by SIRT5 tended to be near glycine, alanine, serine, or threonine residues (Park et al., 2013; Rardin et al., 2013). These differences may be because the substrate binding sites of CPT1A are exposed to the cytosolic side of the mitochondrial outer membrane, while SIRT5 localizes to the mitochondrial matrix. Supporting this reasoning, among 32 mitochondrial CPT1A-dependent lysine-succinylated proteins (32% of the total 101 CPT1A-dependent lysine-succinylated proteins), only 8 proteins were previously identified as potential SIRT5 substrates (Figure 1D; Table S2) (Park et al., 2013).

## CPT1A Is a Regulator of Lysine Succinylation *In Vivo* and Can Lysine-Succinylate Enolase 1 to Inhibit Enolase 1 Activity *In Vitro*

To further examine the role of CPT1A as an LSTase in cells, we knocked down endogenous CPT1A by short hairpin RNA (shRNA) in a breast cancer cell line, T47D cells, which express high levels of CPT1A. We found that CPT1A knockdown (KD) decreased total lysine succinylation levels in lysates (Figure 2A). We further performed SILAC succinyl proteomics analysis using T47D cells with or without stable KD of CPT1A, as similarly performed in 293T cells (Figure 1B). In this case, T47D cells stably transfected with vector control (vector control cells) were incubated with L [U-12C6]-lysine, while T47D cells stably expressing shRNA against CPT1A (CPT1A KD cells) were incubated with H [U-13C6]-lysine. The SILAC succinyl proteomics data showed that succinylation levels of 156 unique lysine sites were decreased by more than 1.3-fold in CPT1A KD cells compared with vector control cells (13% of the total 1,202 detected unique succinyl lysine sites) (Figure 2B; Table S3), suggesting that CPT1A KD caused the overall decrease in lysine succinylation in T47D cells. Furthermore, to verify CPT1A-dependent lysine succinylation in cells, we developed an anti-succinylated lysine motif antibody using a peptide library containing the succinylated motif sequence LVxx(succ)K that we identified using SILAC (Figure 1E). The specificity of this antibody was confirmed by dot blot assay, which showed that the antibody did not recognize acetyl, malonyl, glutaryl lysines, or other acyllysine modifications (Figure 2C). Similar to our findings in Figure 1A, WB with the anti-LVxx(succ)K antibody showed that CPT1A WT expression increased LVxxK succinylation in 293T cells (Figure 2D). Together, these results support the notion that CPT1A is a regulator of lysine succinylation *in vivo*.

We next sought to examine the effects of CPT1A as an LSTase on individual substrate proteins. We focused on enolase 1 because it contained the greatest number of succinylation sites of the 40 proteins identified in our SILAC analysis using CPT1A-expressed 293T cells (Figures S2A and S2B). We ectopically expressed Flag-tagged enolase 1 in 293T cells and showed that CPT1A WT expression increased LVxxK succinylation of immunoprecipitated Flag-tagged enolase 1 compared with expression of the vector control (Figure 3A), confirming our SILAC proteomics data. We further performed WB analysis of two more identified potential CPT1A substrate proteins (creatine

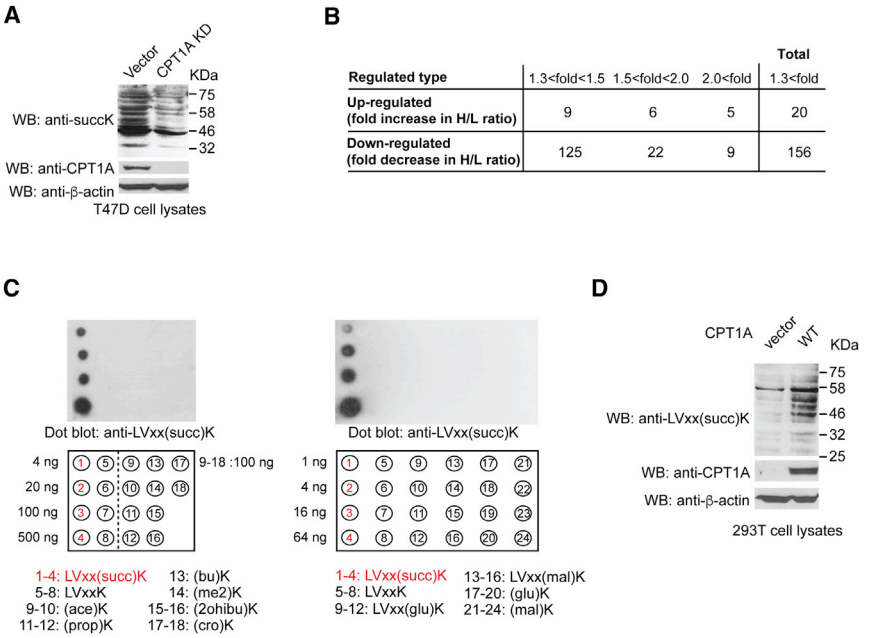


**Figure 2. CPT1A Is a Major Regulator of Lysine Succinylation *In Vivo***

(A) WB of lysates from T47D cells stably expressing vector control and CPT1A shRNA with anti-succinylated lysine, anti-CPT1A, and anti-β-actin antibodies.

(B) Summary of the quantified lysine-succinylated sites in T47D cells with CPT1A KD from SILAC analysis.

(C) Left: dot blotting of unmodified and acylated lysine peptides including succinylated lysine motif LVxx(succ)K, acetyllysine (ace)K, propionyllysine (prop)K, butyryllysine (bu)K, 2-methyllysine (me2)K, 2-hydroxyisobutyryllysine (2ohibu)K, and crotonyllysine (cro)K peptides with anti-LVxx(succ)K antibody. Right: dot blotting of unmodified and succinylated lysine LVxx(succ)K, malonylated lysine LVxx(mal)K, (mal)K, and glutarylated lysine LVxx(glu)K, (glu)K peptides with anti-LVxx(succ)K antibody.

(D) WB of lysates from 293T cells stably expressing vector control and CPT1A WT with anti-LVxx(succ)K succinylated lysine motif, anti-CPT1A, and anti-β-actin antibodies.

See also Figure S2 and Table S3.

kinase B [CKB] and 14-3-3 zeta), one non-target protein that was not detected by our SILAC analysis (glutathione S-transferase [GST]), and one identified protein in which lysine succinylation was decreased by CPT1A expression (histone 4 [H4]). We separately expressed Flag-tagged CKB, GST-tagged 14-3-3 zeta, and GST alone in 293T cells and showed that CPT1A WT expression increased LVxxK succinylation of immunoprecipitated Flag-tagged CKB and pulled down GST-tagged 14-3-3 zeta compared with vector control, but no LVxxK succinylation was observed in pulled-down GST protein alone from 293T cells expressing CPT1A (Figures S3A–S3C). We also showed that CPT1A WT expression decreased K32 succinylation of H4 in 293T cells, but the mechanism of the reduction in H4 K32 succinylation by CPT1A expression remains elusive (Figure S3D). These results together validate the accuracy of our SILAC succinyl proteomics data.

To examine whether CPT1A directly succinylates lysine residues *in vitro*, we purified recombinant CPT1A WT as well as CPT1A H473A, a catalytically inactive mutant that disrupts the putative binding pocket for the sulfur atom of the acyl-CoA thioester (López-Viñas et al., 2007; Morillas et al., 2001, 2004) (Figure S3E). Next, to evaluate the structural properties of purified CPT1A WT and H473A proteins, we examined the relative stability of the CPT1A proteins to limited proteolytic digestion by trypsin as described previously (Kang et al., 2007). Silver staining results showed that there was no obvious difference in the digestion patterns of trypsin-treated CPT1A WT and H473A mutant proteins, suggesting that H473A mutation does not disrupt the overall structure of CPT1A protein (Figure S3F). It is of note that purified CPT1A WT protein, but not purified CPT1A H473A proteins, still possesses the canonical CPTase activity *in vitro* (Figure S3G). We next incubated the purified CPT1A proteins with purified enolase 1 in the presence of 50 μM succinyl-CoA, which is below the physiological concentration of succinyl-CoA in 293T cells (100 μM) (Figure S1B). WB analysis showed that CPT1A WT, but not CPT1A H473A, succinylated enolase 1 on lysines, thus demonstrating that purified CPT1A can directly succinylate enolase 1 *in vitro* and that the H473A mutant lacks LSTase activity (Figure 3B, left). To assess whether lysine succinylation affects enolase 1 catalytic activity, we incubated purified enolase 1 with CPT1A WT and CPT1A H473A and assayed enolase activity. CPT1A WT significantly inhibited enolase 1, whereas CPT1A H473A did not (Figure 3B, right). Together, these results suggest that enolase 1 is a substrate for CPT1A and lysine succinylation of enolase 1 by CPT1A alters enolase 1 catalytic activity. We further performed the *in vitro* succinyltransferase assay to show (1) that BSA, which is a protein that is not a target of CPT1A, is not succinylated (Figure 3C); (2) a time-dependent increase in succinylation on enolase 1 by CPT1A (Figure 3D); and (3) a dose-dependent increase in succinylation on enolase 1 by increased amount of CPT1A (Figure 3E). In addition, we did not observe the time-dependent increase in lysine succinylation of enolase 1 without CPT1A or without succinyl-CoA (Figure S3H) and demonstrated that no lysine succinylation on enolase 1 was induced by CPT1A with malonyl-CoA (Figure S3I).

To further investigate which succinylated lysine sites are responsible for enolase 1 inhibition by CPT1A, we first separately introduced succinylation mimic K-to-E mutations into enolase 1. These mutations included major succinylated lysine sites such as K5, K80, K89, and K233 identified from our SILAC succinyl proteomics data. Although K81 has lowest stoichiometry of succinylation within enolase 1, we introduced K80/81E mutations together because of the proximity of the two sites (Figure S3J). We also introduced another K335E mutation because K335 is proximal to the substrate binding region of enolase 1 (Larsen et al., 1996). We assayed enolase activity of WT, K5 K80/81E, K89E, K233E, and K335E proteins and found that K80/81E and

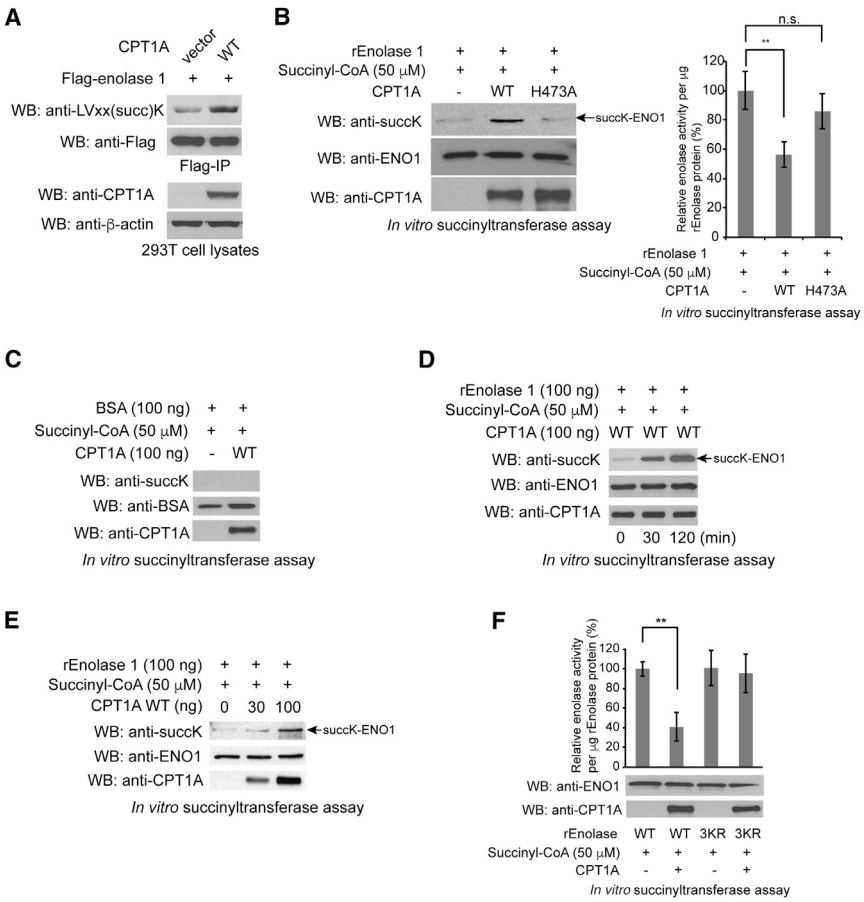


**Figure 3. CPT1A Lysine Succinylates Enolase 1 to Inhibit Its Enzymatic Activity**

(A) Immunoprecipitated Flag-tagged enolase 1 was western blotted with anti-LVxx(succ)K succinylated lysine motif and anti-Flag antibodies. Lysates were western blotted for CPT1A and β-actin.

(B) Left: WB of the *in vitro* succinyltransferase assay samples using purified CPT1A WT or H473A and enolase 1 with anti-pan-succinylated lysine, anti-CPT1A, and anti-enolase 1 antibodies. Right: enolase activity of the *in vitro* succinyltransferase assay samples.

(C) WB of the *in vitro* succinyltransferase assay samples using purified CPT1A WT and BSA with anti-pan-succinylated lysine, anti-CPT1A, and anti-BSA antibodies.

(D) WB of the *in vitro* succinyltransferase assay samples at the indicated time points with anti-pan-succinylated lysine, anti-CPT1A, and anti-enolase 1 antibodies.

(E) WB of the *in vitro* succinyltransferase assay using the indicated amounts of purified CPT1A WT and enolase 1 with anti-pan-succinylated lysine, anti-CPT1A, and anti-enolase 1 antibodies.

(F) Enolase activity of the *in vitro* succinyltransferase assay samples using purified CPT1A WT with enolase 1 WT or 3KR.

Error bars, ±SD of three independent measurements. P values were determined using a two-tailed Student's t test. **p < 0.01; n.s., not significant. See also Figure S3.

K335E mutant exhibited lower enzymatic activity compared with WT, suggesting that K80/81 and K335 succinylation are likely important for the inhibition of enolase 1 by lysine succinylation (Figure S3K). On the basis of these results, we further made succinylation deficient 3KR mutant protein in which all the K80/81 and K335 sites were substituted to Arg (R) and incubated with purified CPT1A WT along with succinyl-CoA and assayed for enolase activity. Purified CPT1A WT did not inhibit the 3KR mutant protein, suggesting that succinylation on K80/81 and K335 is important for CPT1A-dependent inhibition of enolase 1 (Figure 3F). It is of note that the protein sequence surrounding K80/81 of enolase 1 is IAPA(LVSKK)LNVTEQ, which contains the LVxxK motif sequence. In addition, we performed the *in vitro* succinyltransferase assay using purified CPT1A WT and enolase 3KR mutant followed by WB analysis with anti-pan succinyl lysine, anti-CPT1A, and anti-enolase 1 antibodies. The WB results showed that CPT1A did not increase lysine succinylation on enolase 3KR mutant, suggesting that any or all of K80, K81, and K335 are major succinylation sites by CPT1A in the *in vitro* succinyltransferase assay (Figure S3L). Consistent with this finding, we observed that CPT1A KD decreased lysine succinylation of Flag-enolase 1 WT, but not Flag-enolase 1 3KR, compared with vector control in T47D cells (Figure S3M). These results support our notion that endogenous CPT1A can regulate lysine succinylation of enolase 1 in cells.

## Physiological Significance of CPT1A-Dependent Lysine Succinylation in Cells

Because CPT1A H473A lacks both LSTase and CPTase activities (Figures 3B and S3G), we sought a CPT1A mutation that separates LSTase and CPTase activities so that we could assess the impact of selectively disabling the LSTase activity in cells. We found that expression of the previously reported CPTase-deficient mutant CPT1A G710E (Prip-Buus et al., 2001) increased total LVxxK succinylation levels to a similar extent as expression of CPT1A WT in lysates of 293T cells (Figure 4A). We also confirmed that expression of CPT1A WT, but not G710E mutant, increased the CPTase activity in 293T cells compared with expression of vector control although G710E mutant lysine succinylates enolase 1 to a similar extent as CPT1A WT in the *in vitro* succinyltransferase assay (Figures 4B and S3I). G710E mutation was identified from patients with CPT1A deficiency and is a natural mutation that decreases the activity without changing the protein stability (Prip-Buus et al., 2001). Because no crystal structure of CPT1A has been reported yet, a previous study of structure modeling of CPT1A used the crystal structure of mouse carnitine acetyltransferase and showed that G710 is proximal to the catalytic H473 site, and the introduction of a negative charge may impair the catalytic process of the classical CPTase activity of CPT1A by inhibiting the binding of palmitoyl group to the putative substrate binding pocket (Morillas et al., 2004).

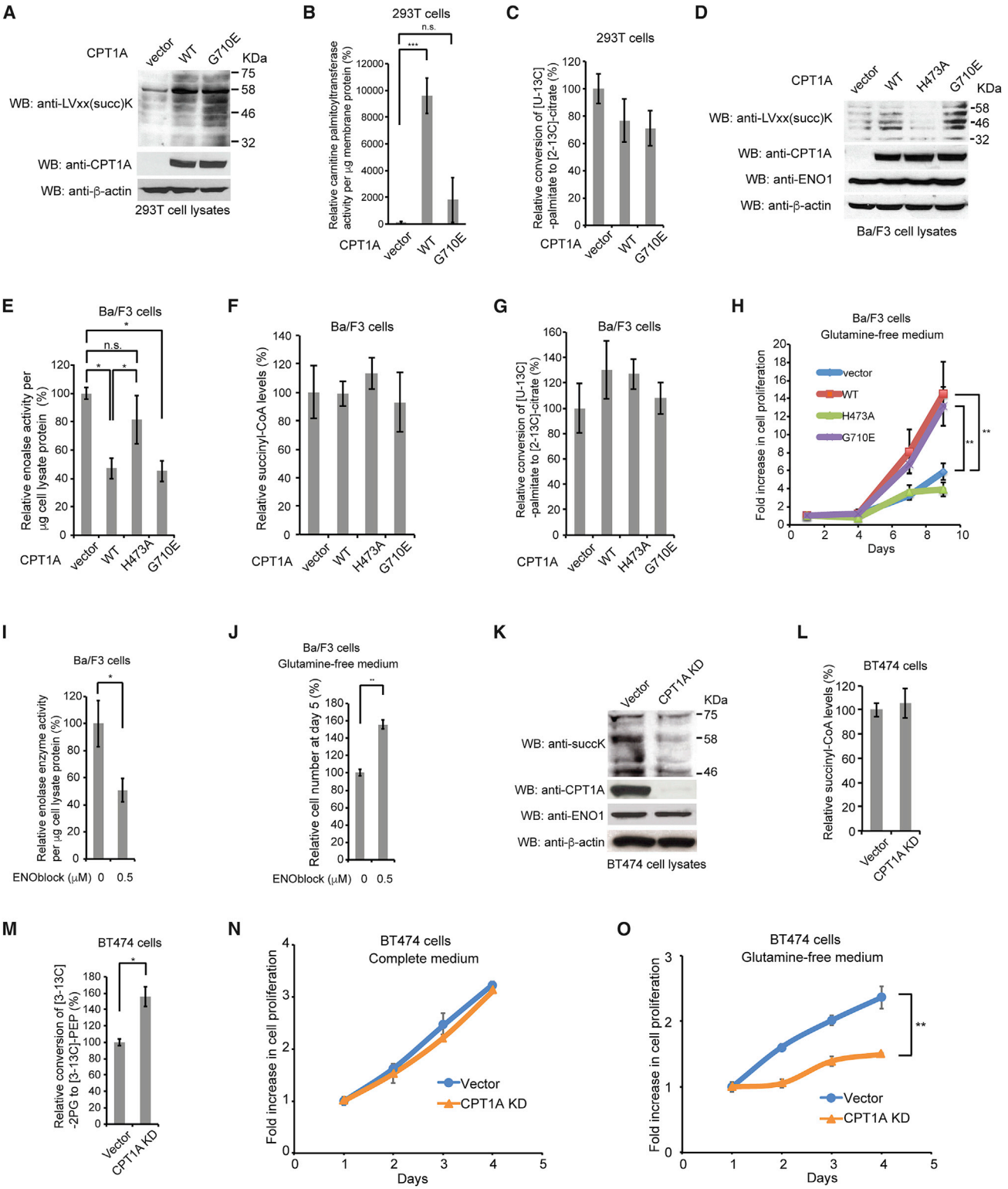


**Figure 4. LSTase Activity of CPT1A Promotes Hematopoietic Cell Proliferation Under Glutamine Depletion**

(A) Lysates from 293T cells stably expressing vector control, CPT1A WT, and CPT1A G710E were western blotted with anti-LVxx(succ)K, anti-CPT1A, and anti-β-actin antibodies.

(B) CPTase activity of membrane proteins from 293T cells stably expressing vector control, CPT1A WT and G710E.

(C) FAO activity in 293T cells expressing vector control, CPT1A WT, and G710E.

*(legend continued on next page)*

We also measured FAO activity in 293T cell lines expressing CPT1A WT and mutants as well as vector control by monitoring the conversion rate of [U-13C]-palmitate to [2-13C]-citrate. We unexpectedly observed no significant alteration of FAO activity by expression of CPT1A WT compared with expression of vector control and CPT1A mutants in 293T cells (Figure 4C). These results may be explained by our finding from the global proteomics data that stable expression of CPT1A WT in 293T cells decreased expression levels of enzymes related to FAO pathway such as very long-chain specific acyl-CoA dehydrogenase (ACADVL), acyl-CoA dehydrogenase family member (ACAD) 9 and 11, 3-ketoacyl-CoA thiolase (ACAA), and 3-hydroxyacyl-CoA dehydrogenase type-2 (HSD17B10), which might decrease the activity of FAO to cancel out the effect of CPT1A WT expression while the mechanism underlying the decrease in expression levels of these proteins remains elusive (Figure S4A; Table S1).

To further ask whether the classical CPTase activity of endogenous CPT1A affects its LSTase activity, we treated breast cancer BT474 cells expressing high levels of endogenous CPT1A with an irreversible inhibitor of CPT1, etomoxir. We found that overnight etomoxir treatment reduced FAO activity to less than 10% but did not affect total LVxxK succinylation levels (Figure S4B). Because KD of CPT1A decreased total succinylation in BT474 cell lysates (Figure 4K), these data together suggest that the CPTase activity and LSTase activity are independently regulated by CPT1A.

The results from Figures 4A and 4B led us to use CPT1A G710E mutant for the following enolase activity assay in cell lysates as well as cell proliferation assay to examine the physiological functions of CPT1A-dependent lysine succinylation in cells. A previous proteomics study showed that among enolase isoforms, only enolase 1-derived peptides were detected in hematopoietic Ba/F3 cells (Pierce et al., 2008), suggesting that enolase 1 is predominantly expressed in Ba/F3 cells, and the total enolase activity in Ba/F3 cell lysates represents the activity of enolase 1. We therefore generated Ba/F3 cells stably expressing vector control, CPT1A WT, CPT1A H473A, and CPT1A G710E and examined the total enolase activity in lysates. Consistent with the results from Figures 3B and 4A, expression of CPT1A WT and CPT1A G710E, but not CPT1A H473A, increased total LVxxK succinylation and inhibited enolase enzyme activity in lysates without altering enolase 1 protein levels compared with vector control (Figures 4D and 4E). Furthermore, consistent with the results from Figures S1B and 4C, we did not observe any significant alteration in intracellular succinyl-CoA levels or FAO activity between these Ba/F3 cell lines (Figures 4F and 4G). Taken together, these results suggest that the LSTase activity, but not the CPTase activity, of CPT1A inhibits enolase in cells.

A recent study showed that shRNA-based silencing of enolase 1 expression induces senescence in breast cancer MDA-MB 231 cells but promotes cell survival under conditions in which glutamine metabolism is suppressed by the glutaminase inhibitor BPTES (bis-2-[5phenylacetamido-1,2,4- thiadiazol-2-yl] ethyl sulfide) (Capello et al., 2016). This led us to test whether the LSTase activity of CPT1A that inhibits enolase 1 may contribute to cell proliferation in glutamine-free medium. We found that CPT1A WT and G710E mutant-expressing Ba/F3 cells, but not H473A mutant-expressing Ba/F3 cells, exhibited increased cell proliferation in glutamine-free medium compared with vector control cells (Figure 4H). There was no significant difference in proliferation of these stable cell lines in complete medium (Figure S4C). Consistent with these results, CPT1A WT and G710E-expressed 293T cells exhibited increased cell proliferation in glutamine-free medium compared with vector control cells (Figure S4D). These results suggest that the LSTase activity, but not the CPTase activity, of CPT1A promotes cell proliferation under glutamine depletion.

To further examine whether the increase in glutamine-independent Ba/F3 cell proliferation by CPT1A WT and by G710E mutant is mediated through enolase inhibition, we treated Ba/F3 cells with an enolase-specific inhibitor, ENOblock, to mimic the inhibition effect of CPT1A on enolase 1 (Jung et al., 2013). We found that 0.5 μM ENOblock treatment reduced enolase 1 activity to a similar extent as in the lysates from CPT1A WT or G710E mutant-expressed Ba/F cells (50% decrease from control treatment or control vector cells) (Figures 4E and 4I). Consistent with our findings, 0.5 μM ENOblock treatment significantly increased cell proliferation in glutamine-free medium but not in complete medium compared with vehicle treatment (Figures 4J and S4E), suggesting that the LSTase activity of CPT1A promotes glutamine-independent Ba/F3 cell proliferation at least in part through the inhibition of enolase. We also performed cell proliferation assay of the

(D) WB of lysates from Ba/F3 cells stably expressing vector control, CPT1A WT, H473A, and G710E with anti-LVxx(succ)K, anti-CPT1A, anti-enolase 1, and anti-β-actin antibodies.
(E) Enolase activity of lysates from Ba/F3 cells stably expressing vector control, CPT1A WT, H473A, and G710E.
(F) GC/MS analysis of succinyl-CoA extracted from Ba/F3 cells expressing vector control, CPT1A WT, H473A, and G710E.
(G) FAO activity in Ba/F3 cells expressing vector control, CPT1A WT, H473A, and G710E.
(H) Glutamine-independent proliferation of Ba/F3 cells stably expressing vector control, CPT1A WT, H473A, and G710E.
(I) Enolase activity of lysates from Ba/F3 cells treated with vehicle control and 0.5 μM ENOblock.
(J) Glutamine-independent proliferation of Ba/F3 cells treated with vehicle control and 0.5 μM ENOblock.
(K) WB of lysates from BT474 cells stably expressing vector control and CPT1A shRNA with anti-succinylated lysine, anti-CPT1A, anti-enolase 1, and anti-β-actin antibodies.
(L) GC/MS analysis of succinyl-CoA extracted from BT474 cells stably expressing vector control and CPT1A shRNA.
(M) GC/MS analysis of enolase activity by measuring the conversion rate of [3-13C]-2PG to [3-13C]-PEP in cells incubated with [U-13C6]-glucose.
(N) Proliferation of BT474 cells expressing vector control and CPT1A shRNA in complete medium.
(O) Proliferation of BT474 cells expressing vector control and CPT1A shRNA in glutamine-free medium.
Error bars, ±SD of three independent measurements. P values were determined by a two-tailed Student's t test. *$p < 0.05$, **$p < 0.01$, ***$p < 0.001$; n.s., not significant. See also Figure S4 and Table S4.

CPT1A-expressed Ba/F3 cell lines treated with etomoxir in glutamine-free medium and found that expression of CPT1A WT and G710E, but not H73A, increased Ba/F3 cell proliferation compared with vector control even in the presence of etomoxir in glutamine-free medium (Figure S4F), suggesting that the growth enhancement observed in glutamine-free medium with expression of CPT1A was not due to the alteration of FAO. We also found no significant alteration in cell proliferation among these Ba/F3 cell lines when treated with AICAR as well as ENOblock and 2-DG in complete medium (Figures S4G and S4H).

To further study the physiological relevance of the LSTase activity of endogenous CPT1A, we sought to examine CPT1A KD BT474 cells of which lysine succinylation levels were decreased in lysates compared with vector control cells (Figure 4K). We confirmed that CPT1A KD did not cause any changes in enolase 1 expression levels and succinyl-CoA levels in BT474 cells (Figures 4K and 4L). It is difficult to assess enolase activity in lysates from BT474 cells with high expression of endogenous SIRT5 compared with other SIRT family members (Table S4), which may desuccinylate enolase to change its activity during cell lysis. To solve this problem, we incubated BT474 cells with [U-13C6]-glucose and measured the conversion rate of [3-13C]-2PG (enolase substrate) to [3-13C]-PEP (enolase product), which represents enolase activity in cells. We found that CPT1A KD cells displayed significantly higher conversion rate of [3-13C]-2PG to [3-13C]-PEP than vector control cells, suggesting that CPT1A KD increased enolase activity in BT474 cells (Figure 4M). To examine whether the observed increase in the total enolase activity by CPT1A KD in BT474 cells is due to changes in enolase 1, we performed total proteomics analysis of BT474 cell lysates. We found that signal intensities from enolase 1-derived peptides were 200 times higher than those from enolase 2-derived peptides, and no other enolase isoforms were detected (Table S4). These results suggest that enolase 1 is predominantly expressed in BT474 cells and the increase in enolase activity by CPT1A KD in BT474 cells is likely due to changes in enolase 1.

Finally, we performed proliferation assays of vector control and CPT1A KD BT474 cells and demonstrated that CPT1A KD significantly decreased cell proliferation in glutamine-free medium but not in complete medium (Figures 4N and 4O). All of the data in Figures 4K–4O are consistent with the other data in Figure 4 and support the notion that the CPT1A increases total lysine succinylation levels without affecting intracellular succinyl-CoA levels to inhibit enolase 1 and enhances glutamine-independent cell proliferation.

Altogether we showed that CPT1A lysine succinylated its substrate proteins *in vivo* and *in vitro*, and such LSTase activity inhibits enolase 1 and promotes cell proliferation under glutamine depletion independent of its classical CPTase activity. These data provide evidence not only for the role of CPT1A as an LSTase but also a functional effect of CPT1A-dependent lysine succinylation on a substrate protein and cellular metabolism. Furthermore, we identified 101 potential CPT1A substrate proteins, expanding the understanding of lysine succinylation-dependent signal transduction in cells. However, it remains unclear how lysine succinylation affects the inhibition of CPT1A by malonyl-CoA, and it also is possible that any alteration in the succinyl-CoA level can regulate the levels of succinylation besides the LSTase activity of CPT1A. Hence, further work would be needed to resolve these issues.

## EXPERIMENTAL PROCEDURES

### Statistical Methods

Significance was tested using unpaired two-tailed Student's t tests, assuming independent variables, normal distribution, and equal variance of samples. Data are presented as mean ± SD from three independent measurements. A p value $< 0.05$ was considered to indicate statistical significance.

### *In Vitro* Succinyltransferase Assay

Purified recombinant CPT1A proteins (100 ng) were incubated with purified recombinant enolase 1 protein (100 ng) at 30°C for 2 hr in 50 μL of the buffer containing 10 mM HEPES (pH 7.5), 2 mM sodium orthovanadate, 5 mM sodium pyrophosphate, 300 mM NaCl, and 1% Nonidet P-40 plus 50 μM succinyl-CoA as a substrate and 50 ng of BSA as a protein stabilizer. The reaction was terminated by the addition of 6xSDS sample buffer and by boiling the samples for 5 min.

### CPTase Activity Assay

CPTase activity was measured using 10 μCi L-[$^3$H]carnitine as previously described (Dobrzyn et al., 2004).

### Metabolic Flux Analysis of FAO

FAO activity was measured by monitoring the conversion rate of [U-13C]-palmitate to [2-13C]-citrate with GC/MS. In brief, the cells were incubated with 100 μM [U-13C]-palmitate-BSA conjugate for overnight. After the incubation, the metabolites were extracted and dried up and then derivatized with MSTFA. The FAO activity was calculated by dividing the citrate labeling rate by the palmitate uptake rate.

### Cell Proliferation Assay

Fold increase in cell proliferation was determined by measuring the cell viability at the indicated days divided by the starting cell viability at day 1 using the CyQUANT Cell Proliferation Assay Kit (Thermo Fisher Scientific).

## DATA AND SOFTWARE AVAILABILITY

The accession number for the proteomics data reported in this paper is PeptideAtlas: PASS01135 (Maxquant_Succinylome293T and Maxquant_SuccinylomeT47D).

## SUPPLEMENTAL INFORMATION

Supplemental Information includes Supplemental Experimental Procedures, four figures, and four tables and can be found with this article online at https://doi.org/10.1016/j.celrep.2018.01.030.

## ACKNOWLEDGMENTS

We thank Dr. Scott Kaufmann for critical reading of the manuscript. We thank Drs. Yuichi Machida and Liewei Wang for providing 293T and T47D cell lines, respectively. We thank Thomas Larson for critical reading of the manuscript. We also thank the Mayo Clinic Cancer Center Pharmacology Shared Resource for providing tissue culture facilities and HPLC analytical expertise. SILAC succinyl proteomics analysis was performed by PTM-Bio. Research reported in this publication was supported by the Career Catalyst Research funding program from the Susan G. Komen Foundation (CCR14300798 to T.H.), the Eagles Cancer Research Fund (T.H.), the Team Science Platform Award from the Mayo Clinic Center for Biomedical Discovery (T.H. and Z.L.), the Developmental Therapeutics Program from the Mayo Clinic Cancer Center (T.H.), and the Mayo Clinic Breast SPORE (P50CA-116201-10 to T.H. and M.P.G.). The content is solely the responsibility of the authors and does not

necessarily represent the official views of the NIH. K.K. and E.K.W. were supported by predoctoral fellowships from the Mayo Foundation for Education and Research. F.B.-A. was supported by NIH Clinical Pharmacology Training Grant T32-GM08685. The Mayo Clinic Cancer Center Pharmacology Shared Resource was supported by NCI Cancer Center Support Grant P30-CA15083-40.

## AUTHOR CONTRIBUTIONS

W.I.G., Z.L., L.M.K., and M.P.G. provided critical equipment, expertise, and reagents. F.B.-A. provided technical assistance for HPLC experiments. K.K., S.H., E.K.W., and T.H. designed the study and performed the experiments. K.K. and T.H. wrote the manuscript. All authors contributed to the discussion of the data.

## DECLARATION OF INTERESTS

The authors declare no competing interests.

Received: August 25, 2017
Revised: December 26, 2017
Accepted: January 9, 2018
Published: February 6, 2018

## REFERENCES

Capello, M., Ferri-Borgogno, S., Riganti, C., Chattaragada, M.S., Principe, M., Roux, C., Zhou, W., Petricoin, E.F., Cappello, P., and Novelli, F. (2016). Targeting the Warburg effect in cancer cells through ENO1 knockdown rescues oxidative phosphorylation and induces growth arrest. Oncotarget *7*, 5598–5612.

Choudhary, C., Weinert, B.T., Nishida, Y., Verdin, E., and Mann, M. (2014). The growing landscape of lysine acetylation links metabolism and cell signalling. Nat. Rev. Mol. Cell Biol. *15*, 536–550.

Colak, G., Xie, Z., Zhu, A.Y., Dai, L., Lu, Z., Zhang, Y., Wan, X., Chen, Y., Cha, Y.H., Lin, H., et al. (2013). Identification of lysine succinylation substrates and the succinylation regulatory enzyme CobB in Escherichia coli. Mol. Cell. Proteomics *12*, 3509–3520.

Dobrzyn, P., Dobrzyn, A., Miyazaki, M., Cohen, P., Asilmaz, E., Hardie, D.G., Friedman, J.M., and Ntambi, J.M. (2004). Stearoyl-CoA desaturase 1 deficiency increases fatty acid oxidation by activating AMP-activated protein kinase in liver. Proc. Natl. Acad. Sci. U S A *101*, 6409–6414.

Du, J., Zhou, Y., Su, X., Yu, J.J., Khan, S., Jiang, H., Kim, J., Woo, J., Kim, J.H., Choi, B.H., et al. (2011). Sirt5 is a NAD-dependent protein lysine demalonylase and desuccinylase. Science *334*, 806–809.

Hitosugi, T., Zhou, L., Elf, S., Fan, J., Kang, H.B., Seo, J.H., Shan, C., Dai, Q., Zhang, L., Xie, J., et al. (2012). Phosphoglycerate mutase 1 coordinates glycolysis and biosynthesis to promote tumor growth. Cancer Cell *22*, 585–600.

Jung, D.W., Kim, W.H., Park, S.H., Lee, J., Kim, J., Su, D., Ha, H.H., Chang, Y.T., and Williams, D.R. (2013). A unique small molecule inhibitor of enolase clarifies its role in fundamental biological processes. ACS Chem. Biol. *8*, 1271–1282.

Kang, S., Dong, S., Gu, T.L., Guo, A., Cohen, M.S., Lonial, S., Khoury, H.J., Fabbro, D., Gilliland, D.G., Bergsagel, P.L., et al. (2007). FGFR3 activates RSK2 to mediate hematopoietic transformation through tyrosine phosphorylation of RSK2 and activation of the MEK/ERK pathway. Cancer Cell *12*, 201–214.

Larsen, T.M., Wedekind, J.E., Rayment, I., and Reed, G.H. (1996). A carboxylate oxygen of the substrate bridges the magnesium ions at the active site of enolase: structure of the yeast enzyme complexed with the equilibrium mixture of 2-phosphoglycerate and phosphoenolpyruvate at 1.8 A resolution. Biochemistry *35*, 4349–4358.

Li, F., He, X., Ye, D., Lin, Y., Yu, H., Yao, C., Huang, L., Zhang, J., Wang, F., Xu, S., et al. (2015). NADP(+)-IDH mutations promote hypersuccinylation that impairs mitochondria respiration and induces apoptosis resistance. Mol. Cell *60*, 661–675.

López-Viñas, E., Bentebibel, A., Gurunathan, C., Morillas, M., de Arriaga, D., Serra, D., Asins, G., Hegardt, F.G., and Gómez-Puertas, P. (2007). Definition by functional and structural analysis of two malonyl-CoA sites in carnitine palmitoyltransferase 1A. J. Biol. Chem. *282*, 18212–18224.

McGarry, J.D., Mannaerts, G.P., and Foster, D.W. (1977). A possible role for malonyl-CoA in the regulation of hepatic fatty acid oxidation and ketogenesis. J. Clin. Invest. *60*, 265–270.

Mills, S.E., Foster, D.W., and McGarry, J.D. (1983). Interaction of malonyl-CoA and related compounds with mitochondria from different rat tissues. Relationship between ligand binding and inhibition of carnitine palmitoyltransferase I. Biochem. J. *214*, 83–91.

Morillas, M., Gómez-Puertas, P., Roca, R., Serra, D., Asins, G., Valencia, A., and Hegardt, F.G. (2001). Structural model of the catalytic core of carnitine palmitoyltransferase I and carnitine octanoyltransferase (COT): mutation of CPT I histidine 473 and alanine 381 and COT alanine 238 impairs the catalytic activity. J. Biol. Chem. *276*, 45001–45008.

Morillas, M., López-Viñas, E., Valencia, A., Serra, D., Gómez-Puertas, P., Hegardt, F.G., and Asins, G. (2004). Structural model of carnitine palmitoyltransferase I based on the carnitine acetyltransferase crystal. Biochem. J. *379*, 777–784.

Park, J., Chen, Y., Tishkoff, D.X., Peng, C., Tan, M., Dai, L., Xie, Z., Zhang, Y., Zwaans, B.M., Skinner, M.E., et al. (2013). SIRT5-mediated lysine desuccinylation impacts diverse metabolic pathways. Mol. Cell *50*, 919–930.

Pierce, A., Unwin, R.D., Evans, C.A., Griffiths, S., Carney, L., Zhang, L., Jaworska, E., Lee, C.F., Blinco, D., Okoniewski, M.J., et al. (2008). Eight-channel iTRAQ enables comparison of the activity of six leukemogenic tyrosine kinases. Mol. Cell. Proteomics *7*, 853–863.

Prip-Buus, C., Thuillier, L., Abadi, N., Prasad, C., Dilling, L., Klasing, J., Demaugre, F., Greenberg, C.R., Haworth, J.C., Droin, V., et al. (2001). Molecular and enzymatic characterization of a unique carnitine palmitoyltransferase 1A mutation in the Hutterite community. Mol. Genet. Metab. *73*, 46–54.

Rardin, M.J., He, W., Nishida, Y., Newman, J.C., Carrico, C., Danielson, S.R., Guo, A., Gut, P., Sahu, A.K., Li, B., et al. (2013). SIRT5 regulates the mitochondrial lysine succinylome and metabolic networks. Cell Metab. *18*, 920–933.

Wagner, G.R., and Payne, R.M. (2013). Widespread and enzyme-independent Nε-acetylation and Nε-succinylation of proteins in the chemical conditions of the mitochondrial matrix. J. Biol. Chem. *288*, 29036–29045.

Weinert, B.T., Schölz, C., Wagner, S.A., Iesmantavicius, V., Su, D., Daniel, J.A., and Choudhary, C. (2013). Lysine succinylation is a frequently occurring modification in prokaryotes and eukaryotes and extensively overlaps with acetylation. Cell Rep. *4*, 842–851.

Zhang, Z., Tan, M., Xie, Z., Dai, L., Chen, Y., and Zhao, Y. (2011). Identification of lysine succinylation as a new post-translational modification. Nat. Chem. Biol. *7*, 58–63.

**Cell Reports, Volume *22***

## Supplemental Information

# Carnitine Palmitoyltransferase 1A

# Has a Lysine Succinyltransferase Activity

**Kiran Kurmi, Sadae Hitosugi, Elizabeth K. Wiese, Felix Boakye-Agyeman, Wilson I. Gonsalves, Zhenkun Lou, Larry M. Karnitz, Matthew P. Goetz, and Taro Hitosugi**

## Supplemental Figures

Figure S1

A

Swiss-Prot search for acyltransferase with coenzyme A binding (33 hits)

Exclude acyltransferases identified in yeast

Potential lysine succinyltransferases (9 hits)

| Entry | Protein names | Gene names |
|---|---|---|
| Q12983 | BCL2/adenovirus E1B 19 kDa protein-interacting protein 3 | BNIP3 NIP3 |
| Q14032 | Bile acid-CoA:amino acid N-acyltransferase (BACAT) (BAT) | BAAT |
| Q8TCG5 | Carnitine O-palmitoyltransferase 1, brain isoform (CPT1-C) | CPT1C CATL1 |
| P50416 | Carnitine O-palmitoyltransferase 1, liver isoform (CPT1-L) | CPT1A CPT1 |
| Q92523 | Carnitine O-palmitoyltransferase 1, muscle isoform (CPT1-M) | CPT1B KIAA1670 |
| P23786 | Carnitine O-palmitoyltransferase 2, mitochondrial | CPT2 |
| Q9Y232 | Chromodomain Y-like protein (CDY-like) | CDYL CDYL1 |
| Q6IB77 | Glycine N-acyltransferase (EC 2.3.1.13) | GLYAT ACGNAT CAT GAT |
| Q9UKG9 | Peroxisomal carnitine O-octanoyltransferase (COT) | CROT COT |

B

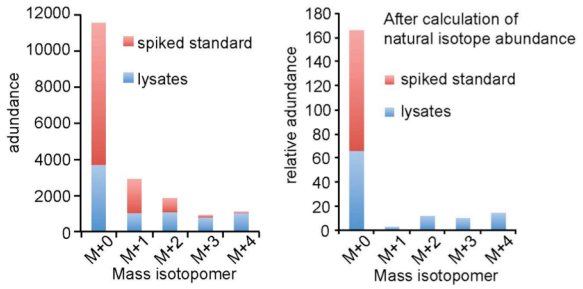


C

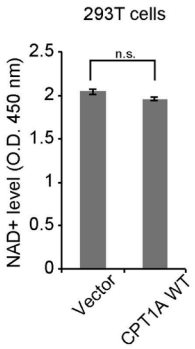


D

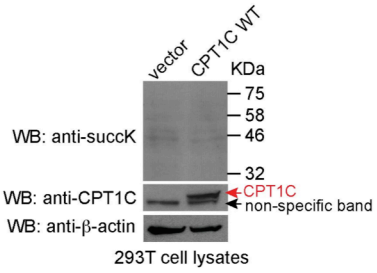


**Figure S1, Screening of potential lysine succinyltranferases, Related to Figure 1.**
(A) Screening for potential lysine succinyltransferases using SWISS-PROT database. (B) *left,* The isotopic distributions of succinate (m/z 289-293; M+0-4) extracted from cell lysates with or without spiking with unlabeled 20 nmoles of succinyl-CoA standard. The cells were incubate with [U-13C]glucose for 12 h before harvest to label endogenous succinyl-CoA. Succniyl-CoA was extracted and purified from the lysates first, and hydrolyzed and detected as succinate by GC/MS as described in Supplemental Experimental Procedures. *right,* The isotopic distributions of the extracted succinate after calculation of natural isotope abundance using IsoPat[2] software with pure succinate standard. Assuming a 200 µL volume for the 293T cell pellet, these figures correlate to intracellular concentrations of 100 µM for succinyl-CoA. (C) The results of NAD+ assay using 293T cells expressing vector control and CPT1A WT. (D) Western blotting results of lysates from 293T cells expressing vector control and CPT1C WT. P values were determined by a two-tailed Student's t test. n.s.: not significant.

Figure S2

A

1. PGK1: K131
2. GAPDH: K61,K194,K215,K263
3. ATB5B: K426
4. ENO1: K5,K64,K71,K80,K81,K89, K228,K233,K330,K335
5. PYGL: K29
6. GPI: K454
7. HSP70: K191,K362,K407
8. HDPD1: K218
9. HSPA: K523
10. ACADM: K217
11. CKB: K242,K307,K313
12. PGAM1: K100
13. TCP1: K400
14. NME2: K124
15. EEF1G: K434
16. CANX: K170
17. STIP: K325
18. CCT6A: K74,K78,K91
19. HADH: K644
20. ACAA2: K234
21. CCT5: K170
22. FACN: K1704
23. PSMB3: K77
24. ACADVL: K278
25. CCT8: K318,K326
26. HSD17B4: K424
27. ACLY: K978
28. HSPE1: K56
29. 14-3-3 zeta: K9,K11,K50
30. RPL1: K67
31. PPIA: K28
32. CLTC: K619
33. PRDX1: K35
34. PTGES3: K33
35. ARAD3B: K364
36. TFG: K103
37. ACO2: K736
38. CACYBP:K8
39. GSTK1: K71
40. MRPL15: K228

B

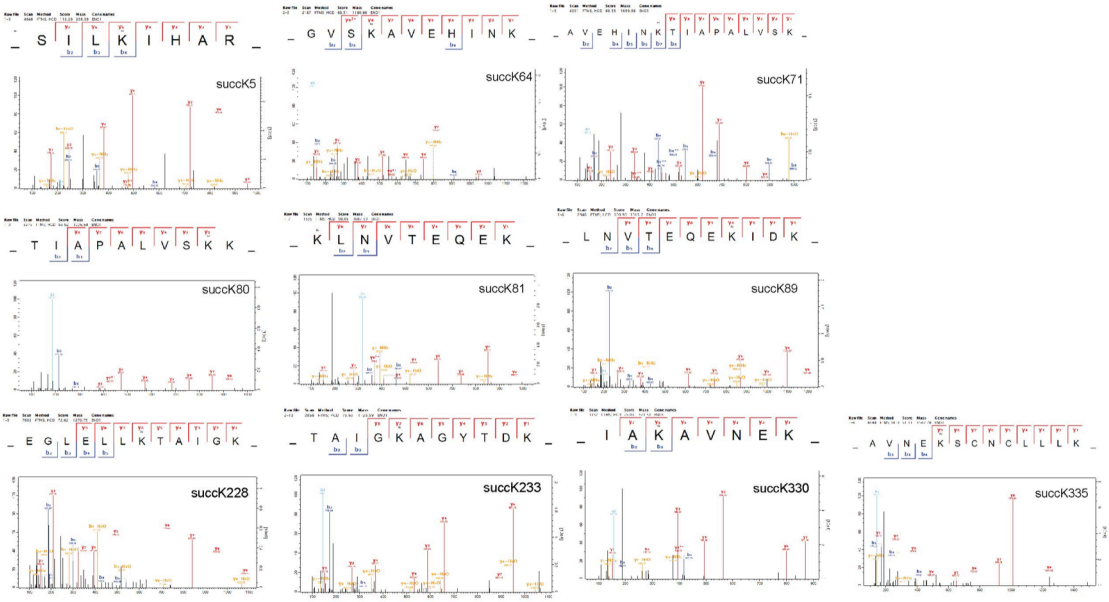


**Figure S2, SILAC succinyl proteomic analysis of cells overexpressing CPT1A, Related to Figure 2.** (A) A list of 40 proteins with succinylated lysine sites that are increased >2.0 fold by CPT1A WT expression in the SILAC-based quantitative lysine succinylation analysis. (B) MS/MS spectrum for the identification and quantification of succinylated enolase 1 peptides. Underlined nominal masses above and below the sequence denote the b and y ions that indicate peptide backbone fragment ions containing the N and C terminal, respectively.

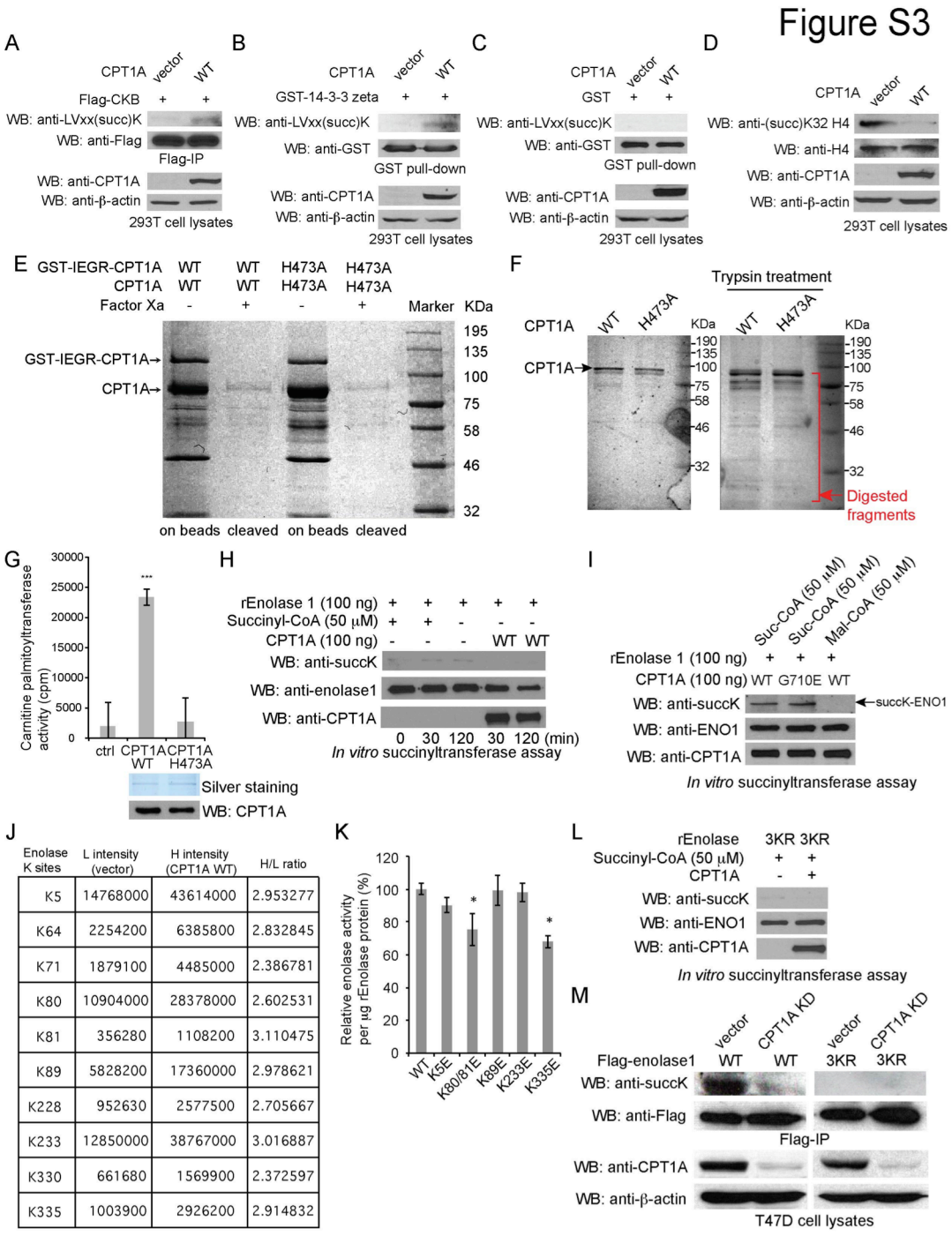


**Figure S3, Validation of SILAC succinyl proteomics analysis, Related to Figure 3.**
(A) Immunoprecipitated Flag-tagged CKB were Western blotted with anti-LVxx(succ)K succinylated lysine motif and anti-Flag antibodies. Lysates were Western blotted for CPT1A and β-actin. (B-C) Pulled down GST-tagged 14-3-3 zeta or GST alone were Western blotted with anti-LVxx(succ)K succinylated lysine motif and anti-GST antibodies. Lysates were Western blotted for CPT1A and β-actin. (D) Western blotting results of lysates from 293T cells stably expressing vector control and CPT1A WT with anti-(succ)K32 H4, anti-H4, anti-CPT1A, and anti-β-actin antibodies. (E) Coomassie blue staining of recombinant CPT1A WT and H473A proteins purified by Factor Xa cleavage. (F) Silver staining of

purified CPT1A WT and H473A proteins treated with or without sequence-grade trypsin (1 unit) for 15 min at room temperature. (G) Carnitine palmitoyltransferase activity assay results of purified CPT1A WT and H473A mutant. Silver staining results and Western blotting results of purified CPT1A proteins with anti-CPT1A antibody are also shown. (H) The *in vitro* succinyltransferase assay was performed using purified enolase 1 and succinyl-CoA without CPT1A protein or using purified CPT1A WT and enolase 1 without succinyl-CoA. The resulting samples were Western blotted with anti-pan-succinylated lysine, anti-CPT1A, and anti-enolase 1 antibodies. (I) The *in vitro* succinyltransferase assay was performed using purified CPT1A (WT or G710E) and enolase 1 with succinyl-CoA or malonyl-CoA. The resulting samples were Western blotted with anti-pan-succinylated lysine, anti-CPT1A, and anti-enolase 1 antibodies. (J) A list of the succinylated lysine sites of enolase 1 along with their peptide peak intensities detected by SILAC succinyl proteomics analysis of 293T cells expressing vector control and CPT1A WT. (K) Enolase activity assay results of purified enolase 1 WT and KE mutants. (L) The *in vitro* succinyltransferase assay was performed using purified CPT1A WT and enolase 1 3KR mutant with succinyl-CoA. The resulting samples were Western blotted with anti-pan-succinylated lysine, anti-CPT1A, and anti-enolase 1 antibodies. (M) Immunoprecipitated Flag-tagged enolase WT and 3KR mutant were Western blotted with anti-pan-succinylated lysine and anti-Flag antibodies. Lysates were Western blotted for CPT1A and β-actin.

A

Figure S4

| Protein names | Gene names | Protein ratio (WT/vector) |
|---|---|---|
| Very long-chain specific acyl-CoA dehydrogenase | ACADVL | 0.64635 |
| Acyl-CoA dehydrogenase family member 11 | ACAD11 | 0.56261 |
| Acyl-CoA dehydrogenase family member 9 | ACAD9 | 0.80496 |
| 3-ketoacyl-CoA thiolase, mitochondrial | ACAA2 | 0.72823 |
| 3-hydroxyacyl-CoA dehydrogenase type-2 | HSD17B10 | 0.81856 |

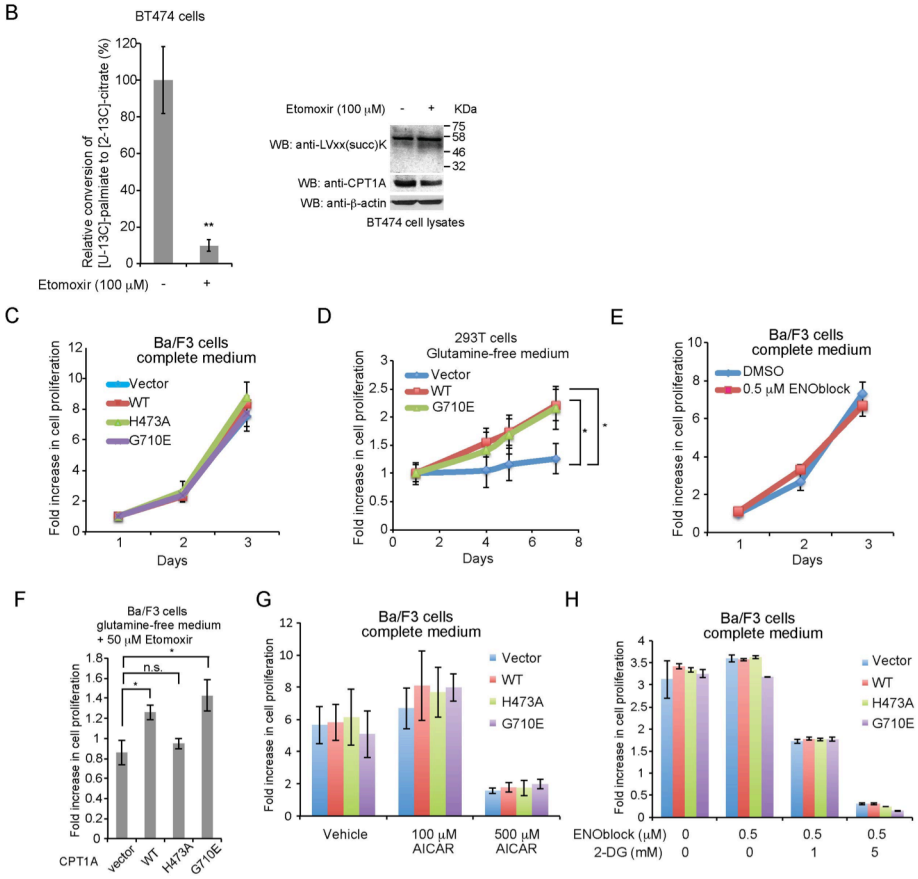


**Figure S4, Functional consequences of CPT1A-dependent lysine succinylation in cells, Related to Figure 4**. (A) A list of enzymes related to fatty acid oxidation pathway whose protein levels were decreased by expression of CPT1A WT in 293T cells. (B) *left,* Metabolic flux analysis of fatty acid oxidation activity in BT474 cells treated with or without etomoxir. *right,* Western blotting results of lysates from etomoxir- or vehicle-treated BT474 cells with anti-LVxx(succ)K, anti-CPT1A, and anti-β-actin antibodies. (C) Proliferation assay results of Ba/F3 cells expressing CPT1A WT and mutants as well as vector control in complete medium. (D) Proliferation assay results of 293T cells expressing CPT1A WT and G710E as well as vector control in glutamine-free medium. (E) Proliferation assay results of Ba/F3 cells treated with 0.5 μM ENOblock and vehicle control in complete medium. (F) Proliferation assay results of Ba/F3 cells expressing CPT1A WT and mutants as well as vector control treated with etomoxir in glutamine-free medium. Cell proliferation was measured at day 5 after the treatment. (G) Proliferation assay results of Ba/F3 cells expressing CPT1A WT and mutants as well as vector control treated with AICAR in complete medium. Cell proliferation was measured at day 2 after the treatment. (H) Proliferation assay results of Ba/F3 cells expressing CPT1A WT and mutants as well as vector control treated with ENOblock and 2-DG in complete medium. Cell proliferation was measured at day 2 after the treatment.

## Supplemental Experimental Procedures

**Cell culture and Western blotting**
293T cells stably transfected with CPT1A WT and mutants were cultured in RPMI 1640 medium with 10% fetal bovine serum (FBS), 1% penicillin/streptomycin, and 100 μg/ml hygromycin. BT474 cells stably transfected with shRNAs against CPT1A were cultured in DMEM/F12 phenol red free medium with 10% FBS, 1% penicillin/streptomycin, and 1 μg/ml puromycin. Ba/F3 cells stably transfected with CPT1A WT and mutants were cultured in RPMI 1640 medium with 10% FBS, 1% penicillin/streptomycin, 10 ng/ml murine IL3, and 1 μg/ml puromycin. 293T and BT474 stable cells were directly lysed, sonicated, and heated at 95°C for 5 min in SDS-PAGE sample buffer containing 10 mM HEPES, pH 7.5, 2 mM sodium orthovanadate, 5 mM sodium fluoride, 5 mM sodium pyrophosphate, 50 mM nicotinamide, 300 mM NaCl, 1% Nonidet P-40, 100 mM dithiothreitol, 5% glycerol, 1% SDS, and cOmplete™ EDTA-free protease inhibitor cocktail (Roche). Ba/F3 cells were lysed in 10 mM HEPES, pH 7.5, 2 mM sodium orthovanadate, 5 mM sodium fluoride, 5 mM sodium pyrophosphate, 50 mM nicotinamide, 300 mM NaCl, 1% Nonidet P-40 and cOmplete™ EDTA-free protease inhibitor cocktail (Roche). Crude lysate was centrifuged at 12,000 x g for 10 min at 4˚C. Clarified lysate was mixed with 6x SDS sample buffer and heated at 95°C for 5 min for Western blotting. The following commercial antibodies were used: anti-pan-succinylated lysine antibody (PTM-401) and anti-succinylated H4 from PTM Bio, anti-β-actin (A1978) and anti-Flag antibodies from Sigma, anti-CPT1A antibody (15184-1-AP) and anti-H4 from Proteintech, and anti-enolase 1 antibody (3810S) from Cell Signaling Technology. Anti-LVxx(succ)K succinylated lysine motif antibody was developed by PTM Bio. All the peptide libraries used for dot blot assay were developed by PTM Bio. ENOblock was purchased from AdoQ bio.

**Anti-Flag immunoprecipiation**
Flag-tagged enolase 1 and CPT1A WT (or vector control) plasmids were transiently co-transfected in 293T cells. Cell lysates were obtained by homogenization in 20 mM HEPES, pH 7.5, 220 mM mannitol, 70 mM sucrose, 1 mM EDTA, 2 mM sodium orthovanadate, 5 mM sodium pyrophosphate, 50 mM nicotinamide, 5 mM dithiothreitol, and cOmplete™ EDTA-free protease inhibitor cocktail (Roche). Crude lysates were centrifuged at 12,000 x g for 10 min at 4˚C. Clarified lysate was diluted with equal volume of 10 mM HEPES, pH 7.5, 2 mM sodium orthovanadate, 5 mM sodium fluoride, 5 mM sodium pyrophosphate, 50 mM nicotinamide, 300 mM NaCl, 1% Nonidet P-40 and then incubated with anti-Flag antibody conjugated beads (Sigma) for 60 min at 4˚C. After the incubation, the beads were washed twice with TBS and the Flag-tagged proteins were eluted with 3X Flag peptide (Sigma) in TBS.

**Retroviral constructs and production of retroviruses.**
Human CPT1A (NM_001876) cDNA was purchased from Genscript. Human enolase 1, 14-3-3, and CKB cDNA were purchased from GE Dharmacon. All cDNAs were amplified by PCR and subcloned into pLHCX-hygro- or pMSCV-puro-derived Gateway destination vector as described (Hitosugi et al., 2012). The pLHCX-hygro destination vectors were co-transfected with packaging plasmids into 293T cells, which were selected in 100 μg/ml hygromycin for 3 weeks. The pMSCV-puro destination vectors were co-transfected with packaging plasmids into 293T cells. Retrovirus was harvested 48 h after transfection, and 8 mg/ml of polybrene was added. Ba/F3 cells were infected with harvested retrovirus and selected in 1 μg/ml puromycin for 2 weeks.

**shRNA constructs and production of lentivirus**
The lentiviral human CPT1A shRNA construct (TRCN0000036279) in the pLKO.1-puro vector was purchased from Open Biosystems. shRNA plasmids were co-transfected into 293T cells along with lentiviral packaging plasmids as described (Hitosugi et al., 2012). Lentivirus was harvested 48 h after transfection, and 8 μg/ml of polybrene was added. Subconfluent BT474 cells were infected with harvested lentivirus and selected in 1 μg/ml puromycin for 2 weeks.

**Site-directed mutagenesis**

H473A and G710E mutations were introduced into CPT1A using a QuikChange-XL site-directed mutagenesis kit (Stratagene). All constructs were sequence verified using Sanger sequencing.

**SILAC labeling and sample preparation for LC-MS/MS analysis**

SILAC labeling was performed using SILAC Protein Quantification Kit (Pierce, Thermo) according to the supplier's instructions. The signal intensity of a lysine succinylated peptide with heavy (H) $^{13}C_6$ lysine labeling was divided by that with light (L) $^{12}C_6$ lysine labeling to calculate the lysine succinylation H/L ratio (Figure 1B). To accurately quantify CPT1A-dependent succinylation levels of each lysine site, the lysine succinylation H/L ratio on each peptide was normalized by the peptide H/L ratio, which was calculated by dividing the peptide counts of the corresponding peptide with heavy (H) $^{13}C_6$ lysine labeling by those with light (L) $^{12}C_6$ lysine labeling detected by the quantitative LC-MS analysis. 293T cells expressing CPT1A-WT were labeled with $_L$- $^{13}$C-Lysine (heavy amino acid), while the control 293T cells expressing pLHCX vector were labeled with $_L$-$^{12}$C Lysine (light amino acid). The labelings were performed separately and the cells were passaged at least six times to ensure 97% labeling efficiency before harvest. The cells were expanded in SILAC media to obtain ~5 x $10^8$ cells, collected and washed twice with ice-cold PBS supplemented with 3 μM trichostatin A (TSA) and 50 mM nicotinamide (NAM). The cell pellets were sonicated three times using high intensity ultrasonic processor (Scientz) in NETN buffer (150 mM NaCl, 1 mM EDTA, 20 mM Tris, pH 8.0 and 0.5% NP-40) containing 5 mM DTT, 3 μM TSA, 1% protease inhibitor cocktail III, 2 mM EDTA and 50 mM NAM in addition to 8 M urea. Equal amounts of crude proteins from "heavy" and "light" labeled cells were mixed and precipitated with 15% trichloroacetic acid (TCA). The precipitated proteins were washed twice with -20˚C acetone, dissolved in 100 mM $NH_4HCO_3$, pH 8.0 and digested with trypsin at a trypsin-to-protein ratio of 1:50 (w/w) at 37˚C for 16 h. Following digestion, DTT was added to a final concentration of 5 mM. The samples were incubated at 50˚C for 30 min and alkylated using iodoacetamide (Sigma) at a final concentration of 15 mM at room temperature in the dark for 30 min. The alkylation reaction was quenched using 30 mM cysteine at room temperature for 30 min, and the samples were further digested by adding trypsin at a ratio of 1:100 (w/w) at 37˚C for 4 h. The digested peptide samples were separated into 18 fractions by using a C18 column (Agilent 300Extend C18 column, 250 x 4.6 mm, 5-μm particle size) using a gradient of 2% to 60% acetonitrile (ACN) in 10 mM ammonium bicarbonate, pH 10.0, over the period of 80 min. To enrich the lysine succinylated peptides, the tryptic peptides were first dissolved in NETN buffer and then incubated with anti-pan-succinylated lysine antibody-conjugated beads (PTM Bio) at 4˚C overnight with gentle shaking. The beads were washed four times with NETN buffer and twice with $ddH_2O$. The bound peptides were eluted from the beads by using 0.1% trifluoacetic acid (Sigma). The eluted fractions were combined, vacuum-dried and further cleaned with C18 ZipTips (Millipore) according to the supplier's instructions.

**LC-MS/MS succinyl proteomics analyses and database searching**

Enriched peptides were dissolved in 0.1% formic acid (Fluka) and directly loaded onto a reversed-phase analytical column (Acclaim PepMap RSLC, Thermo Scientific) equipped with a pre-column (Acclaim PepMap 100). Peptides were separated with a constant flow rate of 300 nl/min on an EASY-nLC 1000 UPLC system with a gradient composed of solvent B (0.1% formic acid in 98% ACN). The method was run from 6% to 22% solvent B for the first 26 min, 22% to 35% for 8 min and then to 80% in a 3 min duration and a final 3 min hold at 80%. The MS/MS analysis was performed on a Q Exactive™ Plus hybrid quadrupole-Orbitrap mass spectrometer (ThermoFisher Scientific) using a nanospray ionization (NSI) source. For MS scans, the m/z scan range was from 350 to 1800 and the intact peptides were detected in the Orbitrap at a resolution of 70,000. Peptides were selected for MS/MS using NCE setting as 30; ion fragments were detected in the Orbitrap at a resolution of 17,500. A data-dependent procedure that alternated between one MS scan followed by 20 MS/MS scans was applied for the top 20 precursor ions above a threshold ion count of 1E4 in the MS survey scan with 10.0 s dynamic exclusion. The electrospray voltage applied was 2.0 kV and automatic gain control (AGC) was used to prevent overfilling of the ion trap; 5E4 ions were accumulated for generation of MS/MS spectra. The resulting MS/MS data was processed using MaxQuant with integrated Andromeda search engine (v.1.4.1.2). Tandem mass spectra were searched against *SwissProt_Human* (20,274 sequences) database concatenated with reverse decoy database. Mass error was set to 10 ppm for precursor ions and 0.02 Da for fragment ions. False discovery rate (FDR) thresholds for protein, peptide and modification site were specified at 1% while the minimum peptide was set at 7. All the other parameters in the MaxQuant were set to default values. The site localization probability was set as >0.75. We normalized our whole proteomics data by the customary

calculation that divides all the signal intensity values by the average value, which is necessary to normalize the data based on the sample loading amount. While in succinyl proteomics, sample preparation with enrichment of succinylated peptides by immunoprecipitation should result in a difference in the total amount of succinylated peptides between the vector and CPT1A KD samples because CPT1A KD cells showed significant decrease in lysine succinylation in lysates as compared to vector control cells as shown in Figure 2A. This difference in the total amount of succinylated peptides makes the different averages of the signal intensities from succinylated peptides in vector control and CPT1A KD cells, and such different averages should represent biologically relevant difference in succinylation between vector control and CPT1A KD cells (the average of signal intensities from succinylated peptides in CPT1A KD cells divided by that in vector cells was 0.88 as shown in Table S3, suggesting that overall succinylation is decreased by CPT1A knockdown as expected from Western blotting results in Figure 2A) and should not be directly used for the customary calculation to normalize succinyl proteomics data. Instead, we performed the following two-step normalization for our succinyl proteomics data in Figure 2B as previously published (Hebert et al., 2013; Park et al., 2013): **1)** We normalized our succinyl proteomics data by the customary calculation using T47D whole proteomics data (all the numbers of the signal intensities from succinylated peptides in vector control and CPT1A KD cells were respectively divided by the average of the signal intensities from the "total peptides" in vector control and CPT1A KD cells, which enables to normalize the succinyl proteomics data based on the starting amount of the total peptides in vector control and CPT1A KD cells); **2)** We further divided the "H/L ratios" of succinylated peptides from step **1** by the "H/L ratios" of total peptides, which were taken from the same cell lysates as illustrated in Figure 1. This additional normalization makes sure that changes in H/L ratio are due to changes in lysine succinylation on each protein, not due to changes in its protein expression or experimental artifacts from incomplete incorporation of heavy amino acids into cells. We also normalized the succinyl proteomics data from 293T cells in Figure 1 in the exactly same way.

**Purification of recombinant CPT1A proteins**

CPT1A proteins were purified using Factor Xa Cleavage Capture kit (Millipore) since neither of N-terminus nor C-terminus Flag-tagged CPT1A proteins showed any enzymatic activities (data not shown). The CPT1A variants with N-terminus Factor Xa cleavage sequence (IEGR) and the CPT1A variants without the IEGR sequence were respectively subcloned into pDEST27 (N-terminus GST-tag) destination vector and pcDNA 3.2 (no tag) Gateway destination vector (Life Technologies). GST-IEGR-CPT1A WT along with CPT1A WT (or GST-IEGR-CPT1A H473A mutant along with CPT1A H473A mutant) were co-transfected into 293T cells. Transfected 293T cells were lysed in buffer containing 10 mM HEPES, pH 7.5, 2 mM sodium orthovanadate, 5 mM sodium fluoride, 5 mM sodium pyrophosphate, 300 mM NaCl, 1% Nonidet P-40, and protease inhibitor cocktail (Roche). GST-IEGR-CPT1A and CPT1A proteins were pulled down from the lysates by glutathione-Sepharose beads. The GST-IEGR-CPT1A and CPT1A protein bound beads were extensively washed with PBS and treated by Factor Xa enzyme in PBS to obtain cleaved CPT1A proteins. Factor Xa was removed by Factor Xa Cleavage Capture kit. The purification efficiency was examined by Coomassie blue staining.

**Purification of recombinant enolase 1**

Human enolase 1 (BC011130) cDNA (GE Dharmacon) was amplified by PCR and subcloned into pET53 Gateway destination vector, which appends an N-terminal $His_6$-tag, as described (Hitosugi et al., 2012). Transformed BL21(DE3)pLysS *E. coli* were grown to a density of 0.5 (OD600) at 37˚C and induced with 1 mM IPTG for 4 h at 37˚C. Bacterial cells were collected and sonicated in buffer containing 20 mM sodium phosphate, pH 8.0 0.5 M NaCl, and 20 mM imidazole in the presence of protease inhibitor and centrifuged at 4,800 x g for 15 min at 4˚C. Clarified lysate was loaded onto a Ni-NTA column and washed with 20 mM sodium phosphate, pH 8.0 and 0.5 M NaCl, and 20 mM imidazole. Bound proteins were eluted with 20 mM sodium phosphate, pH 8.0 and 0.5 M NaCl, and 250 mM imidazole. Proteins were desalted on a PD-10 column and purity of the preparation was assessed by Coomassie blue staining.

***In vitro* enolase activity assay**

Enolase activity was measured using an enzyme coupled assay. Enolase enzyme mix containing 100 mM Tris-HCl, pH 7.5, 100 mM KCl, 5 mM $MgCl_2$, 1 mM ADP, 0.2 mM NADH, 0.5 unit/ml recombinant human pyruvate kinase M1 purified as described (Hitosugi et al., 2012), and 0.1 unit/ml rabbit muscle lactate dehydrogenase (EMD Millipore) was prepared. 2-phosphoglycerate (2-PG) was added last to initiate

the reaction at a final concentration of 2 mM. The decrease in autofluorescence (ex: 340 nm, em: 460 nm) due to NADH oxidation was measured as enolase activity. The reaction mixtures of *in vitro* succinyltransferase assay were directly used for the enolase activity assay. For the activity assay of enolase in Ba/F3 cells, cells were lysed in 10 mM HEPES, pH 7.5, 2 mM sodium orthovanadate, 5 mM sodium pyrophosphate, 300 mM NaCl, 1% Nonidet P-40 and protease inhibitor cocktails. Crude lysate was centrifuged at 12,000 x g for 10 min at 4˚C. Clarified lysate was used for enolase enzyme activity assay.

**Carnitine palmitoyltransferase activity assay**

Carnitine palmitoyltransferase activity was measured as described (Dobrzyn et al., 2004). Cells were homogenized in buffer containing 20 mM HEPES, pH 7.5, 220 mM mannitol, 70 mM sucrose, 1 mM EDTA, 10 μM PMSF, 10 mM EGTA, 2 mM sodium orthovanadate, 5 mM sodium fluoride, and 5 mM sodium pyrophosphate. The homogenates were centrifuged at 1,000 x g for 10 min at 4°C to remove nuclear material and cell debris. The supernatant was further centrifuged at 14,000 x g for 5 min at 4°C to obtain membrane proteins. 200 μg of the membrane proteins were added to the assay medium containing 20 mM HEPES, pH 7.5, 75 mM KCl, 1% BSA, 4 mM $MgCl_2$, 4 mM ATP, 250 μM GSH, 70 μM palmitoyl-CoA, 0.25 mM carnitine, 10 μCi L-[$^3$H]carnitine, with or without 100 μM malonyl-CoA. Samples were incubated at 37°C for 10 min. The reaction was stopped by the addition of 0.5 ml of ice-cold 1 M perchloric acid. The reaction mixtures were centrifuged and the supernatant was removed. The membrane pellets were resuspended in 0.5 ml of $ddH_2O$ and extracted with 0.6 ml of 1-butanol. 0.4 ml of the 1-butanol phase was back-extracted with 60 μL of $ddH_2O$. Seventy microliters of the 1-butanol-phase was counted by liquid scintillation and malonyl-CoA-sensitive carnitine palmitoyltransferase activity was calculated.

**GC/MS analysis of succinyl-CoA**

Intracellular levels of succinyl-CoA in cell lines expressing CPT1A WT and mutants as well as vector control were measured with an isotope-ratio based approach using GC/MS as we have performed previously (Hitosugi et al., 2012). In brief, two dishes of cells were cultured in media supplemented with [U-13C]glucose for 12 hours to label endogenous succinyl-CoA first, one dish of cells were quickly rinsed in ice-cold PBS and homogenized in 10% TCA, and same number of cells in another dish were also quickly rinsed in ice-cold PBS and homogenized in 10% TCA spiked with 80 nmoles of pure succinyl-CoA standard (Sigma). The homogenates were centrifuged to remove debris and the resulting supernatants were applied to a solid-phase extraction column preconditioned with methanol followed by water. The columns were washed with water three times, and succinyl-CoA was eluted with methanol. The eluents were dried up and reconstituted in water. The succinyl-CoA solution was made alkaline with NaOH to hydrolyze succinyl-CoA at 40$^o$C for 1 hour and acidified with HCl. Succinate was extracted from the acidified solutions with ethylacetate, derivatized with MTBSTFA in DMF, and analyzed by GC/MS (Li et al., 2015). The detailed isotopic distributions of succinate extracted from cell lysates with or without spiking with unlabeled succinyl-CoA standard were presented in Figure S4A. The change in isotopic distribution of the extracted succinate (m/z 289-293) by spiking with unlabeled succinyl-CoA standard was measured to quantify intracellular endogenous succinyl-CoA levels. Natural isotope abundance was calculated with IsoPat$^2$ software using pure succinate (Gruber et al., 2007).

**NAD+ quantification assay**

Intracellular NAD+ levels were measured by a NAD+/NADH colorimetric kit (BioVision) as per manufacturer's instructions. Briefly, metabolites were extracted from 2 x $10^5$ of 293T cells expressing CPT1A WT (or vector control) with freeze/thaw cycles in the extraction buffer. 1/4 of the extracted sample was used for total NAD+ and NADH detection and the rest samples were heated at 60 $^o$C for 30 min to decompose all the NAD+. The samples were then mixed in the NAD cycling enzyme mix for 5 min at room temperature and incubated with NADH developer for 1-2 hours at room temperature. Total NAD+ and NADH as well as NADH were separately measured by $OD_{450nm}$. The concentration of NAD+ was then calculated by subtracting the NADH value from the total NAD+ and NADH.

**GC/MS analysis of enolase activity by measuring the conversion rate of [3-13C]-2PG to [3-13C]-PEP in cells incubated with 13C-glucose**

Enolase activity was measured by monitoring the conversion rate of [3-13C]-2PG to [3-13C]-PEP with GC/MS. In brief, the cells were incubated with [U-13C]-glucose for overnight. After the incubation, the

cells were quickly rinsed in ice-cold PBS and lysed with 50% methanol. The crude lysates were centrifuged to remove debris. The resulting supernatants were dried with nitrogen gas, derivatized with MSTFA, and then injected onto GC/MS as previously described (Hitosugi et al., 2012). The flux rate of [U-13C]-glucose to [3-13C]-2PG was determined by dividing the ion intensity of [3-13C]-2PG (m/z 462) by that of [12C]-2PG (m/z 459) and the flux rate of [U-13C]-glucose to [3-13C]-PEP was determined by dividing the ion intensity of [3-13C]-PEP (m/z 372) by that of [12C]-PEP (m/z 369). The enolase activity was calculated by dividing the [3-13C]-PEP flux rate by the [3-13C]-2PG flux rate.

## Supplemental References


Dobrzyn, P., Dobrzyn, A., Miyazaki, M., Cohen, P., Asilmaz, E., Hardie, D. G., Friedman, J. M. and Ntambi, J. M. (2004). Stearoyl-CoA desaturase 1 deficiency increases fatty acid oxidation by activating AMP-activated protein kinase in liver. *Proc Natl Acad Sci USA* 101, 6409-6414.

Gruber, C. C., Oberdorfer, G., Voss, C. V., Kremsner, J. M., Kappe, C. O. and Kroutil, W. (2007). An algorithm for the deconvolution of mass spectroscopic patterns in isotope labeling studies. Evaluation for the hydrogen-deuterium exchange reaction in ketones. *J Org Chem* 72, 5778-83.

Hebert, A. S., Dittenhafer-Reed, K. E., Yu, W., Bailey, D. J., Selen, E. S., Boersma, M. D., Carson, J. J., Tonelli, M., Balloon, A. J., Higbee, A. J. et al. (2013). Calorie restriction and SIRT3 trigger global reprogramming of the mitochondrial protein acetylome. *Mol Cell* 49, 186-99.

Hitosugi, T., Zhou, L., Elf, S., Fan, J., Kang, H. B., Seo, J. H., Shan, C., Dai, Q., Zhang, L., Xie, J. et al. (2012). Phosphoglycerate mutase 1 coordinates glycolysis and biosynthesis to promote tumor growth. *Cancer Cell* 22, 585-600.

Li, F., He, X., Ye, D., Lin, Y., Yu, H., Yao, C., Huang, L., Zhang, J., Wang, F., Xu, S. et al. (2015). NADP(+)-IDH Mutations Promote Hypersuccinylation that Impairs Mitochondria Respiration and Induces Apoptosis Resistance. *Mol Cell* 60, 661-75.

Park, J., Chen, Y., Tishkoff, D. X., Peng, C., Tan, M., Dai, L., Xie, Z., Zhang, Y., Zwaans, B. M., Skinner, M. E. et al. (2013). SIRT5-mediated lysine desuccinylation impacts diverse metabolic pathways. *Mol Cell* 50, 919-30.

Pizer, E. S., Thupari, J., Han, W. F., Pinn, M. L., Chrest, F. J., Frehywot, G. L., Townsend, C. A. and Kuhajda, F. P. (2000). Malonyl-coenzyme-A is a potential mediator of cytotoxicity induced by fatty-acid synthase inhibition in human breast cancer cells and xenografts. *Cancer Res* 60, 213-8.

Tsuchiya, Y., Pham, U., Hu, W., Ohnuma, S. and Gout, I. (2014). Changes in acetyl CoA levels during the early embryonic development of Xenopus laevis. *PLoS One* 9, e97693.